Effect of Solar Collector Area and Storage Tank Capacity on the Performance of the Absorption Chiller

Mohamed H. Ahmed*‡

*Solar Energy Department, National Research Centre, Cairo 12622, Egypt

‡ Corresponding Author; Mohamed H. Ahmed, 33 El Buhouth St. Dokki, Tel: +20 100 529 1830

mo555as@hotmail.com

Received: 12.01.2020 Accepted:18.02.2020

Abstract- Recently, solar cooling has received great attention as the demand for cooling complies with the availability of solar radiation. While solar radiation is variable throughout the day, the need to use a suitable storage system is necessary. Determining the area of the solar collector and the storage capacity is an important issue for solar thermal applications. In this study, the effect of different design parameters such as the solar collector area and the storage tank capacity for the solar absorption cooling system of 30 kW were investigated. Also, the effect of the hot water temperature entering the absorption chiller on the ratio of the cooling energy gained to the nominal cooling capacity was studied. The TRNSYS simulation program was implemented to simulate the thermal performance of the solar absorption cooling systems in the summer period in Cairo, Egypt. The theoretical results of the simulation proved that increasing the solar collector surface area from 20 to 200 m^2 increased the operating period of the absorption chiller from 2.9 to 11.5 h in June. While increasing the storage tank capacity from 2 to 4 m^3 reduced the outlet hot water temperature from the storage tank. This reduction varies throughout the day time. Increasing the inlet water temperature to the absorption chiller from 90 to 125 ºC raises the ratio of cooling gained to the chiller nominal capacity from 74 to 87 % at a chilled water setpoint temperature of 3 ºC and from 90 to 99 % at setpoint temperature of 12 °C. This improvement depends on the setting temperature of the outlet chilled water.

Keywords Solar collector, storage tank, adsorption chiller, simulation, TRNSYS.

1. Introduction

Cooling and air conditioning consume the most electric energy produced in hot countries. In Egypt, the household sector consumed electric energy for cooling and air-conditioning by about 32% of the total electricity generated [1]. Solar cooling is the use of heat energy collected from solar radiation to operate heat-operated refrigeration and air-conditioning unit. Solar thermal energy is collected by solar collectors of various types, and then this heat is pumped through heat transfer fluids (water or oil) to the cooling units, which in turn are given cold water or air that is used to cool and conditioning the buildings. The solar cooling systems contain three main parts, the first part are the solar collector, which converts the sun's radiation into heat energy, the second part is the cooling unit, and the third part is a source of heat expulsion, often a cooling tower.

Many companies have developed, manufactured and marketed sorption refrigeration systems, whether they depend on absorption or adsorption of different sizes, due to their relatively good performance compared to other refrigeration systems [2]. The absorption and adsorption cooling systems are comparable in terms of performance but the adsorption system is more expansive due to the high volume of components required for the same capacity. Researchers carried out several investigations on the performance of the adsorption cooling system, Ahmed et al presented a theoretical and experimental investigation of solar adsorption cooling unit with single bed using zeolite and water as working pair, their reach maximum COP of 0.4 at inlet hot oil temperature of about 174 ºC [3]. The biggest disadvantage of the adsorption system is the high initial cost (1000 € /kW) [4]. The advantage of using solar energy to operate adsorption chillers is the very low electrical energy consumed compared to conventional cooling systems. Using

solar thermal energy to power the cooling and air conditioning system leads to save fossil fuel consumption and reduce the emissions CO_2 and other gases harmful to the environment. Also, the uses of other refrigerants such as CFCs, which harmful to the environment, are absent in these alternative ways. The absorption cooling process includes the same processes as in the vapour compression cooling system, where it includes the vapour compression process, the heat rejection process (condensation), expansion process, and evaporation process. In the absorption cooling system, the refrigerants used are ammonia, lithium bromide or water. The refrigerant is condensed inside the condenser where the heat is expelled, while the cooling effect occurs inside the evaporator, where the refrigerant liquid evaporates withdrawing the heat from the surrounding medium. The parametric analysis and energy of solar absorption cooling systems during different climatic conditions for Morocco were investigated by Agrouaz et al [5]. The results of their study presented the best configuration design for the solar absorption cooling system. It was found that increasing the capacity of the storage tank from 0.5 to 3 m^3 has no effect on the solar fraction where the increase in the solar fraction doesn't exceed 3 %.

Much research has been conducted regarding absorption cooling systems (ACS) in dynamic conditions. A simulation program for the thermal performance of a single-effect absorption cooling system that is driven by solar energy for two different configurations, using the Transient System Simulation program (TRNSYS) has been built by Ahmed et al [6]. In the first configuration C_1, the heating fluid coming from the generator of the absorption chiller (AC) flows completely to the hot storage tank. While in the second configuration C_2, the heating fluid coming from the absorption chiller bypassed the storage tank when the fluid in the tank has a temperature lower than required and flows directly to a backup heater. The results proved that the second configuration leads to a noticeable saving in energy compared to the first configuration for the whole summer season. Al-Alili et al [7] assessed the feasibility of using solar evacuated tube collector to drive 10 kWc ammonia-water absorption chiller. Based on the thermal analysis, the solar air conditioner system has a specific collector area of 6 m^2/kWc and a specific tank volume of 0.1 m^3/kWc. The selected system size requires about 47% less electrical energy than the vapor-compression cycles of the same capacity. Absorption chiller unit driven by solar energy was analyzed by Stanciu et al. [8]. The thermal energy provided to the generator coming from a hot water storage tank that connected with a fixed oriented solar parabolic trough collector. From the output results, the longest period of continuous operation of the NH_3-H_2O cooling system, from 09:00 AM to 5:10 PM, was achieved at 2.9 m parabola width and 10 m parabola length and with a 0.16 m^3 storage tank capacity. The previous results were predicted at a corresponding evaporator temperature of about 10 ºC. Different system configuration to operate the absorption chiller for a complete day was investigated by Al-Ugla et al. [9]. The study aimed to find the most suitable configuration. They concluded that a system design with refrigerant storage of a solar LiBr/H_2O absorption system is the best choice where it achieves a high COP of 0.77 with a solar collector surface area of 22 m² compared to other system configurations. Atif Saeed et al. [10] developed and fabricated a prototype of Ammonia water single stage absorption refrigeration system to replace the traditional air conditioning system with the absorption system which consumes less electric energy. Use solar energy to operate the refrigeration unit was investigated with different solar collectors. The evacuated tube collector was used to operate a LiBr/H_2O single-effect absorption chiller, hot water storage and an auxiliary heater by Naranjo-Mendoza et al [11]. Comparisons between different solar collector types were done by several researchers [12-14]. Tao He et al. [15] presented a new solar thermal cooling system powered by an evacuated tube collector (ETC). The system has been modelled by TRNSYS software. They have concluded that for a 50 ton refrigeration unit the optimum tank size is 15 m^3 and 8 m^3 in the case of heating and cooling, respectively. Mazloumi et al. [16] developed a model to simulate a LiBr/H_2O absorption chiller with a nominal cooling capacity of 17.5 kW coupled with a parabolic trough collector (PTC). They obtained the minimum required collector area and the optimum storage tank capacity for various flow rates within the collector loop. The results showed that the collector mass flow rate has a negligible effect on the minimum required collector area, while it has a significant effect on the optimal capacity of the storage tank. Florides et al. [17] developed a simulation program of solar absorption cooling system with 11 kW cooling capacity. The results showed that the optimum system consisted of 15 m^2 PTC with a 600 L hot water storage tank. Agyenim et al. [18] carried out an experimental test on a LiBr/H_2O absorption chiller with 12 m^2 ETC and 1 m^3 water storage tank to store cold water generated instead of hot water. The authors concluded that when there was excessive solar radiation, and at a targeted cold water temperature between 7 and 10 °C, a storage size between 180 and 250 L was required for every kW of chilled water produced.

The solar Linear Fresnel Reflector (LFR) was selected in the present work for its advantage over the other solar concentrators in terms of achieving a very low Levelized Cost of Energy (LCOE). The aim of the present work is to model and simulate a complete solar absorption cooling system consists of Linear Fresnel Reflector, a stratified storage tank and a single-effect absorption chiller based on LiBr/H_2O as working fluid. A tempering valve was inserted between the absorption chiller and the storage tank to control the inlet hot water temperature to the absorption chiller. The simulation program investigates the effect of the LFR collector area on the operating period of the absorption chiller and the chilled energy produced by the chiller. The study also includes the use of Linear Fresnel Reflector as a solar heat collector and investigates its visibility on powering an absorption chiller. The effect of the inlet hot water temperature on the fraction of the nominal capacity of the absorption chiller was investigated. A TRNSYS simulation program, version 17, was used for carrying out the simulation of the solar cooling system. In addition to TRNSYS types, some types of Thermal Energy System Specialists (TESS) were used in the simulation.

2. Description of the System

The solar absorption cooling system consists of three main loops connected together to form the solar cooling system as shown in Fig.1. The heat transfer fluid in the whole loops is pressurized water. The first loop is the solar heating cycle, it consists of LFR solar collector, a circulating pump, and a stratified storage tank. A differential controller device was inserted in the solar loop to control the water flow rate of this loop. The second loop is the AC powering loop, it consists of a storage tank, the absorption chiller, circulating pump, tempering controller, Tee pieces distributer and Tee piece mixture. The third loop is the load loop; it consists of the absorption chiller, circulating pump, and the load. The operating and design parameters of the different system components are illustrated in table 1.

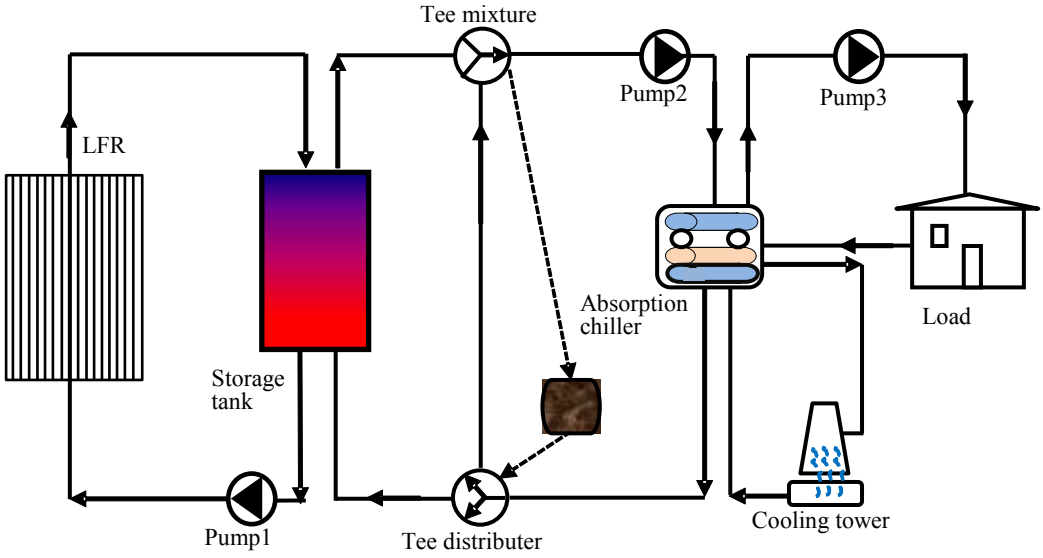

Fig. 1. A schematic diagram of the solar absorption cooling system

Table 1. The input parameters for the TRNSYS program

Items	Quantity	Unit
Solar collector type	LFR	-
Solar collector area	20-200	m^2
Storage tank capacity	2-4	m^3
Absorption chiller capacity	30	kW
Max. chiller driving temperature	125	ºC
Chilled water set point	6-12	ºC
Cooling load	25	kW
Solar loop flow rate	2	kg/s
Hot water flow rate	1.8	kg/s
Cooling water flow rate	5.1	kg/s
Chilled water flow rate	1.6	kg/s
Hot & cold water Specific heat	4.18	kJ/kg k
Tank specified	Stratified	-
Weather data	TM2, Cairo	-

3. Simulation Model

The thermal performance of the solar absorption cooling system is investigated by a simulation model. The TRNSYS program was used for this purpose. A schematic diagram of the TRNSYS components that form the solar absorption cooling system in the TRNSYS simulation platform is shown in Fig.2. The components (types) include the linear Fresnel Reflector, storage tank, absorption chiller, cooling tower, load, pumps, and controllers. All these components are connected together where the outputs from each component are the inputs for the next components. The different component models used in the simulation are described in the following sections.

3.1. Linear Fresnel Reflector

This component model simulates the performance of linear Fresnel reflector. This model has been widely used both for testing and simulation. The collector heat energy balance equation from the quasi-dynamic methodology presented in Standard EN12975-2 was used in modeling the LFR collector. The full terms equation of the collector model for the collector useful output power $\dot{Q}_u$ is written as [19]:

$$\begin{aligned}\dot{Q}_u &= F(\tau\alpha)_{en}\,k_{\theta b}(\theta)G_b + F(\tau\alpha)_{en}\,k_{\theta d}(\theta)G_d - C_6uG \\ &\quad - C_1(T_m - T_a) - C_2(T_m - T_a)^2 - C_3u(T_m - T_a) \\ &\quad + C_4(E_L - \sigma T_a^4) + C_5(dT_m/dt)\end{aligned} \qquad (1)$$

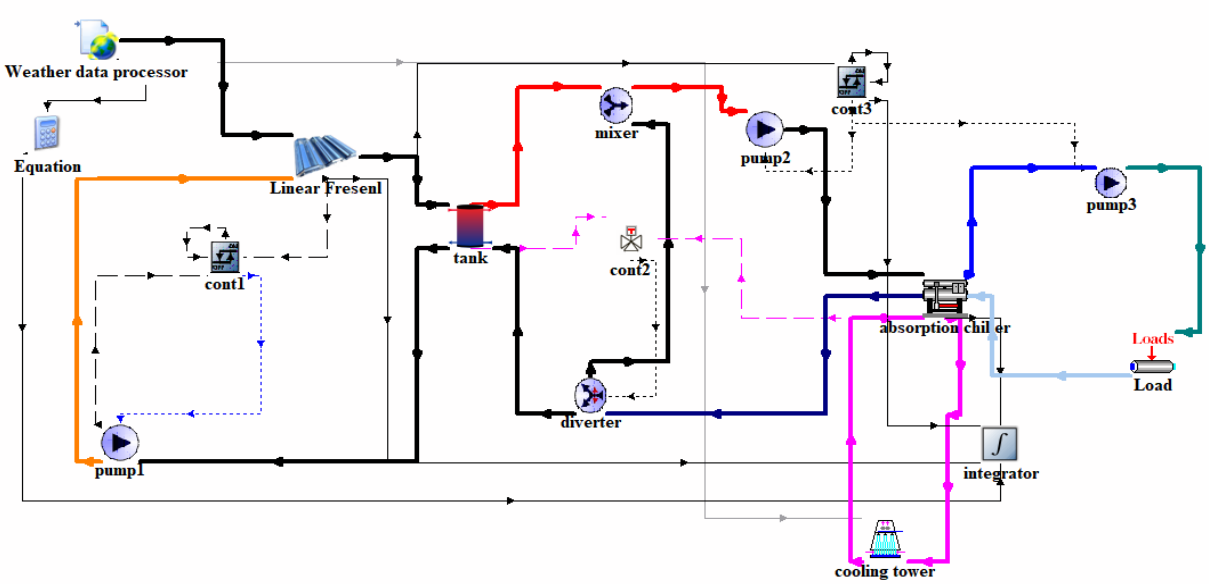

Fig. 2. The TRNSYS model of the solar absorption system in the simulation studio

Where $F(\tau\alpha)_{en}$ is the zero loss efficiency, C_1 and C_2 terms represent the temperature dependence of the heat loss coefficient, C_3 and C_4 represent the heat loss coefficients depending on the wind speed and sky temperatures respectively, C_5 and C_6 is the effective thermal capacity and wind speed dependence of the zero-loss coefficient respectively. E_L, G, u, k, and σ are the longwave irradiance, solar irradiance, wind speed, the incidence angle modifier, and Stefan–Boltzmann constant, respectively.

3.2. Stratified Storage Tank

This model of type 4 simulates the thermal performance of a fluid-filled sensible energy storage tank, subjected to thermal stratification. The stratification of modeled in this work depended on assuming that the tank consists of 75 fully-mixed equal volume segments. This component model a stratified tank having fixed inlet positions defined within the code. Fluid entering the cold side of the tank enters the bottom node. While the fluid entering the hot side of the tank is added to the top tank node. This instance assumes that losses from each tank node are equal. The energy balance equation for the i^{th} segment is presented as following [20]:

$$M_i Cp_f \frac{dT_i}{dt} = \alpha_i \dot{m}_h Cp_{h,f}(T_h - T_i) + \beta_i \dot{m}_c Cp_{c,f}(T_c - T_i) + UA_i(T_{amb} - T_i) + \dot{Q} + \gamma_i Cp_f(T_{i-1} - T_i) + \gamma_i Cp_f(T_i - T_{i+1}) \quad (2)$$

Where $\dot{m}_h$ and $\dot{m}_L$ are the mass flow rates for hot and cold fluids, respectively. M_i is the mass of fluid in segment i, $Cp_{h,f}$ and $Cp_{c,f}$ are the specific heat of the hot and cold fluid respectively. T_h, T_c, and T_i are the hot, cold and segment fluid temperature. α_i, β_i, and γ_i are control functions. UA_i is the overall heat loss coefficient of one segment.

3.3. Controlled Flow Diverter

This component of the Type 11f model simulates a flow diverter, mode 2, in which a single inlet liquid stream is divided into two liquid streams, according to an input signal ranges from 0 to 1, this signal comes from the tempering controller. The function of this component is to pass a part of the hot liquid that returned from the absorption chiller at a lower temperature ($T_{hw,ch,o}$) to the mixer. This part mixes through a mixer with the hotter liquid coming out of the tank and destined to the refrigeration unit to reduce the temperature of the liquid going to the absorption chillier to a specified value set by the controller. This is done when the temperature of the hot fluid coming from the storage tank ($T_{hw,st,o}$) and going to the absorption chiller is greater than required.

3.4. Tempering Valve Controller

This component calculates the fraction of fluid that should be sent to the mixer. The controller calculates the amount of fluid that should be flow into the storage tank and the amount of fluid bypassing the storage tank that, when mixed together with hot stream exit from the tank, provides the setpoint temperature (T_{set}). The fraction (λ) of the fluid bypassed the storage tank is given by:

$$\lambda = 1 - \frac{T_{set} - T_{hw,ch,o}}{T_{hw,st,o} - T_{hw,ch,o}} \quad (3)$$

3.5. Tee Piece

This component of the Type 11h simulates a tee piece, mode 1, in which two inlet liquid streams are mixed together into a single liquid outlet stream. The temperature of the mixed hot water streams delivered into the absorption chiller ($T_{hw,ch,i}$) is given by:

$$T_{hw,ch,i} = \frac{\dot{m}_{st,o} T_{hw,st,o} - \dot{m}_{pas,} T_{hw,ch,o}}{\dot{m}_{st,o} + \dot{m}_{pas}} \quad (4)$$

Where $\dot{m}_{st,o}$ is the flow rate of hot water stream exit the storage tank, $\dot{m}_{pas}$ is the flow rate of the bypassed hot water that mixed with hot water coming from the storage tank.

3.6. Single-Effect Absorption Chiller

This component of the Type107 utilizes a table lookup method to simulate the thermal performance of an absorption chiller powered by hot water. The absorption chiller in this type is a single effect. In the absorption unit, the refrigerant, which is water, evaporates in the evaporator then the vapor flows to a solution of lithium bromide and water where the vapor is absorbed by the solution and condenses into liquid, heat is generated as a result of the absorption process. Cooling water stream is used to cool the solution and get rid of the heat generated. The diluted solution is supplied to the generator, in this device the heat transfer from the hot water into the solution to take out (desorb) the refrigerant. Then the water vapor flows into the condenser to lose its heat and then flows through an expansion valve to the evaporator as a liquid. Type107 uses the previous technique to estimate the performance of the absorption unit. In this absorption chiller type, the chiller is designed to cool a third fluid stream to a required setpoint temperature. The model calculates the value of energy that removed from the chilled water stream $\dot{Q}_{chw}$ to reduce its temperature to the setpoint value:

$$\dot{Q}_{chw} = \dot{m}_{chw} CP_{chw} (T_{chw,in} - T_{chw,out}) \quad (5)$$

Where $T_{chw,in}$ and $T_{chw,out}$ are the inlet and outlet chilled water temperatures of the absorption chiller. The heat energy supplied to the generator of the absorption unit by the hot water $\dot{Q}_{hw}$ was calculated from the following equation:

$$\dot{Q}_{hw} = \dot{m}_{hw} CP_{hw} (T_{hw,i} - T_{hw,o}) \quad (6)$$

Where $T_{hw,in}$ and $T_{hw,out}$ are the temperatures of the inlet and outlet hot water stream. The energy expelled to the cooling water fluid $\dot{Q}_{cw}$ is predicted by the following equation:

$$\dot{Q}_{cw} = \dot{Q}_{Chw} + \dot{Q}_{hw} + \dot{Q}_{aux} \quad (7)$$

Where $\dot{Q}_{aux}$ represents the total electric energy consumed by the different devices inside the absorption chiller such as pumps, controls,…etc. The outlet temperature of the cooling water $T_{cw,o}$ stream can be calculated from the following equation:

$$T_{cw,o} = T_{cw,i} + \frac{\dot{Q}_{cw}}{\dot{m}_{cw} Cp_{cw}} \quad (8)$$

The COP of the absorption chiller can be calculated from the following equation:

$$COP = \frac{\dot{Q}_{chw}}{\dot{Q}_{hw} + \dot{Q}_{aux}} \quad (9)$$

3.7. Heating load

This model simply imposes a specified load on a flowing stream and calculates the resultant outlet fluid conditions. Type682 can be thought of as an interaction point between a building load and the liquid working fluid in an HVAC system. Mathematically, this model is very simple. The necessary parameters include the flow rate, specific heat, and temperature of the liquid at a point in the system loop that should be provided. The building loads are added to, or subtracted from that liquid, resulting in an outlet temperature just past the interaction point.

$$T_{L,out} = T_{L,in} + \frac{\dot{Q}_L}{\dot{m}_{chw}\ Cp} \quad (10)$$

Where $\dot{Q}_L$ is the cooling load, $T_{L,in}$ and $T_{L,out}$ is the inlet and outlet chilled water to the load, respectively.

3.8. Weather Data

Weather data is introduced using type 15-6 metronome file TM2 for Cairo, Egypt having a latitude and longitude of 30º 1' and 31º 14', respectively.

4. Simulation Result and Discussion

In this section, the result of the simulation program for the solar absorption cooling system will be presented for different solar collector areas through the summer months. The effect of the storage tank capacity on the chiller performance will be also investigated. The TRNSYS simulation program was run at 15 minutes time step.

The ambient temperature for Cairo through the investigation period, from the first of April to the end of September, is illustrated in Fig.3, where the maximum ambient temperature ranges from 35 to 39 ºC. The instantaneous global solar radiation and Direct Normal Irradiance (DNI) are presented throughout the same period in Fig.4. It can be observed that the maximum total solar radiation and beam radiation has been recorded in June and July, where the maximum total radiation ranges from 880 to 1000 W/m^2 and the maximum DNI ranges from 710 to 820 W/m^2 as its ratio to the total radiation fluctuate around 81 %.

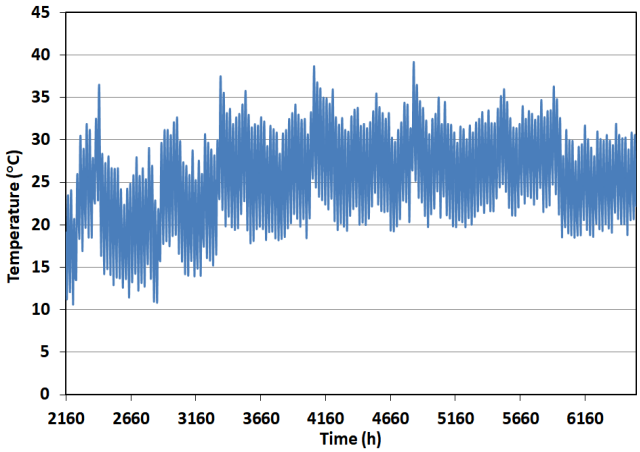

Fig. 3. The ambient temperature through the summer months in Cairo

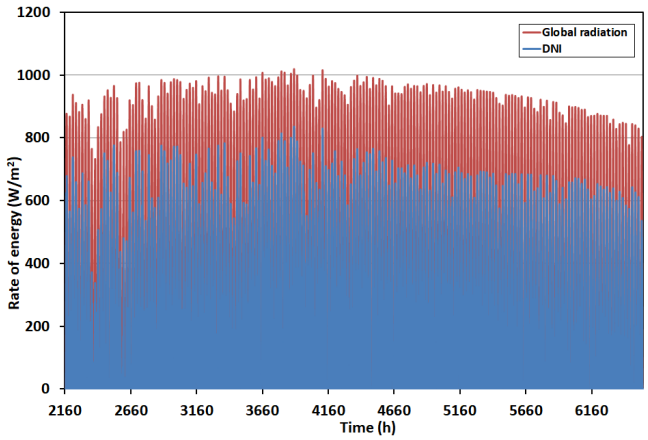

Fig. 4. Global and Direct Normal Irradiance through the summer months in Cairo

The monthly chilled energy produced by the absorption chiller is affected by the solar collector surface area of the Linear Fresnel Reflector. Figure 5 presents this effect at different summer months. The months of April, May, and June were selected to present the summer period where the other months, from July to September, give symmetric results. It can be seen from the figure that, increasing the LFR surface area from 20 to 140 m^2 leads to an increase in the chilled energy produced from 4.5 to 25 GJ in April and from 8.13 to 31.1 GJ in June. The increase in the chilled energy can be attributed to the high outlet water temperature from collector consequently the high collected energy. Also increasing the collector surface area leads to an increase in the operating period of the absorption chiller as shown in Fig.6.

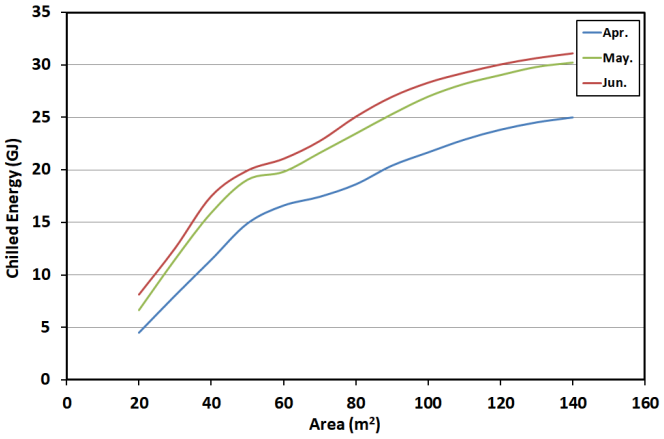

Fig. 5. Variation of the monthly chilled energy vs the solar collector area at summer months

The effect of increasing the solar collector surface area on the operating period of the absorption chiller is illustrated in Fig. 6 for three summer months. Increasing the surface area of the LFR from 20 to 200 m^2 leads to an increase in the daily operating period from 1.64 h which is a very low period to 9.24 h in April, and increases the daily operating period from 2.9 to 11.5 h in June. Increasing the LFR collector more than 140 m^2 has no notable effect on the operating period for the same storage tank capacity.

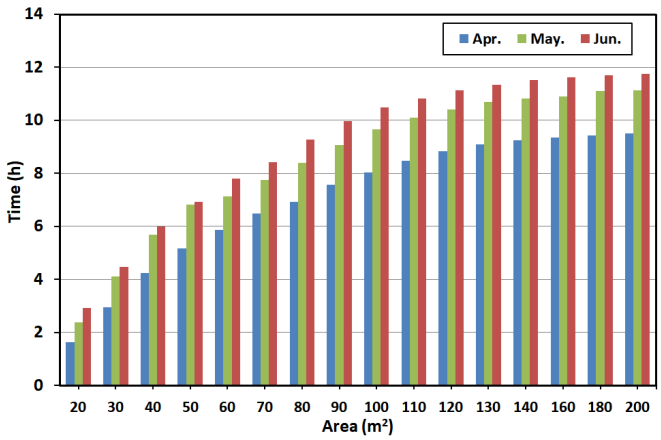

Fig. 6. The operation period of the absorption chiller versus the solar collector area for three summer months

The inlet hot water temperature to the absorption chiller has an effect on the fraction of the nominal chiller capacity. Figure 7 shows this effect at different setpoint temperatures for the outlet chilled water. The cooling energy fraction of chiller nominal capacity has a constant value with increasing the inlet hot water temperatures from 90 up to 105 ºC, and then the fraction increase gradually with increasing the hot water temperature until a value of 120 ºC, then it became constant again for higher inlet hot water temperature. The cooling fraction increases from 0.74 to 0.87 for T_{set} equal to 3 ºC, while for T_{set} of 12 ºC, the cooling fraction increases from 0.9 to 0.99. It can be seen also that increase the setting value of the outlet chilled water temperature increase the fraction of the chilled energy produced by the absorption chiller.

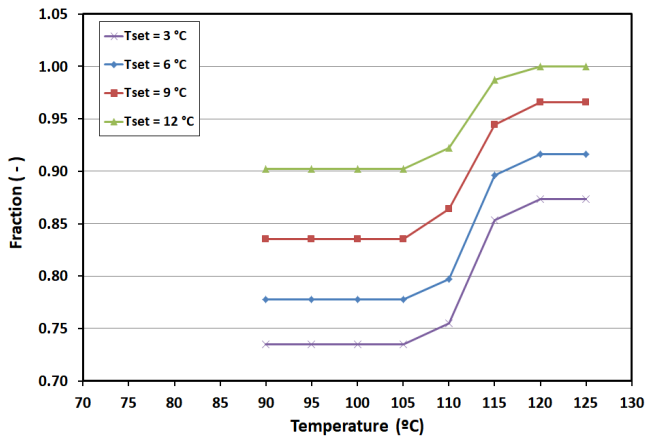

Fig. 7. Effect of the inlet hot water temperature on the fraction of chiller capacity at a different set point temperature of chilled water

The inlet and outlet hot water temperature of the absorption chiller is shown in Fig.8 at two different solar collector surface areas. At a solar collector area of 120 m^2, the difference between the inlet and outlet fluid temperature ranges from 6.3 to 7 ºC. While for the solar collector area of 140 m^2, the difference between the inlet and outlet fluid temperature for the solar LFR is ranges from 6.6 to 7.5 ºC.

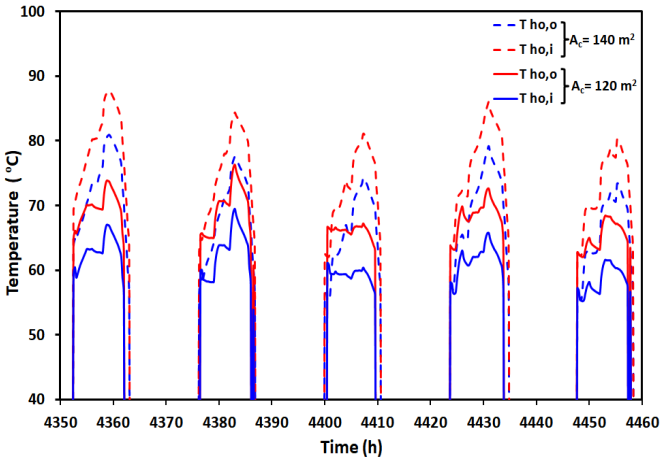

Fig. 8. The inlet and outlet temperature of the hot water to the absorption chiller at two solar collector areas

The effect of the solar collector area on the inlet hot water temperature to the absorption chiller is illustrated in Figs. 9 and 10 for storage tank capacities of 2 and 4 m^3, respectively. From Fig.9, the effect of the solar collector area on the inlet temperature is shown for one day in summer, it can be seen that the maximum allowable inlet temperature to the absorption chiller was set to 95 ºC and the minimum allowable temperature was set at 62 ºC. From the figure, it can be observed that with increasing the collector area from 80 to 200 m^2 the inlet hot water temperature and also the operating time of AC increases. The operation of the AC starts from 8 to 8:30 AM and ends from 5:30 to 7:25 PM, depending on the collector area. For the collector surface areas of 180 and 200 m^2, the inlet hot water temperature reaches its maximum allowable value for a certain period, 3.75 and 5 hours respectively. While for storage tank capacity of 4 m^3, the inlet hot water temperature to the absorption chiller doesn't reach the maximum allowable value as shown in Fig. 10. Therefore, no amount of returning hot water from the absorption chiller is directed to the mixing valve.

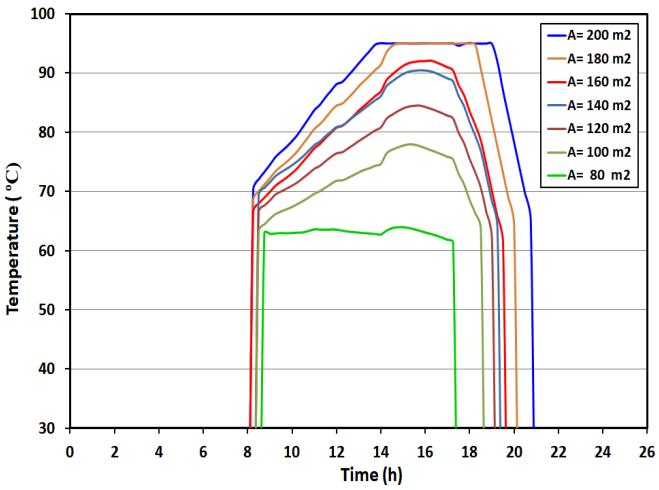

Fig. 9. Effect of the solar LFR area on the inlet hot water temperature to the absorption chiller at 2 m^3 storage capacity and different collector surface areas

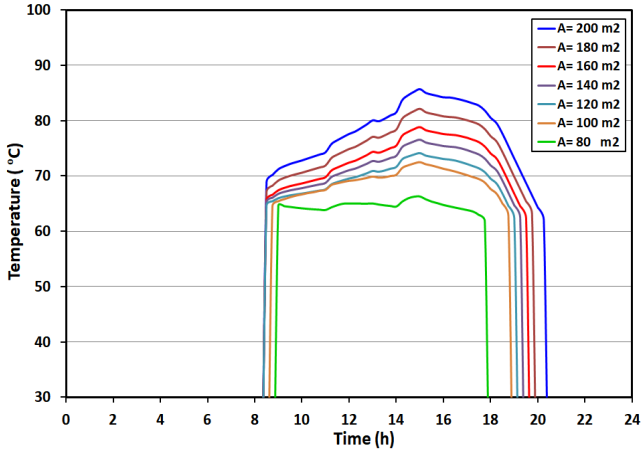

Fig. 10. Effect of the solar LFR area on the inlet hot water temperature to the absorption chiller at 4 m^3 storage capacity

5. Conclusion

This paper investigates the effect of the solar collector surface area and storage tank capacity on the thermal performance of the solar absorption cooling system in terms of the operating period of the chiller, the cooling energy fraction of the nominal chiller capacity, and the chilled energy. The TRNSYS simulation program, version 17, was used to carry out this investigation. The simulation carried out under the Cairo climate (30 ° N). The results of this simulation proved that increasing the collector surface area from 20 to 200 m^2 increase the daily operation period from 2.9 to 11.5 h for June. The outlet water temperature from the LFR solar collector is affected by the collector surface area, as increasing the collector area from 120 to 140 m^2 leads to an increase in the maximum temperature of the outlet hot water from 73.7 to 87.1 ºC, respectively. This observation affects the collector temperature rise, as the increase in the outlet water temperature of the solar collector leads to increase the temperature of the water returning from the absorption chiller then the inlet water temperature supplied to the solar collector, which results in a decrease in the temperature rise through the collector. The temperature rise through the LFR decreases from 7.1 ºC to 6.8 ºC as a result of increasing the inlet water temperature from 67 ºC to 80 ºC. Increasing the chiller inlet hot water temperature leads to an increase in the output power fraction of the chiller capacity. This increase depends on the setting temperature of the outlet chilled water. At a setpoint temperature of 3 ºC, increasing the entering hot water temperature from 90 to 125 ºC leads to an increase in the cooling energy fraction of the nominal capacity of the absorption chiller from 74 to 87 %. While at setpoint temperature of 12 ºC, the fraction of the nominal capacity was increased from 90 to 99 %, respectively. Increasing the storage tank capacity from 2 to 4 m^3 reduces the hot water temperature entering the absorption chiller, this reduction varying according to the solar collector area.

References

[1] A. Elsafty and A. J. Al-Daini, “Economical comparison between a solar-powered vapour absorption air-

conditioning system and a vapour compression system in the Middle East", Renewable Energy, Vol. 25, No. 4, pp. 569-583, 2002.

[2] A. Allouhi, T. Kousksou, A. Jamil, Y. Agrouaz, T. Bouhal, R. Saidur, and A. Benbassou, "Performance evaluation of solar adsorption cooling systems for vaccine preservation in Sub-Saharan Africa", Applied Energy, Vol. 170, pp. 232-241, May 2016.

[3] M. H. Ahmed, H. H. El-Ghetany, A. A. Abdel Aziz, and A. E. Zohir "Modeling and Performance Prediction of an Adsorption Cooling System with Single Bed", International Journal of Renewable Energy Research, Vol. 8, No. 4, pp. 2156–2166, 2018.

[4] D. S. Kim and C. A. Infante Ferreira, "Solar refrigeration options – a state of the art review", International journal of refrigeration, Vol. 31, No. 1, pp. 3-15, January 2008.

[5] Y. Agrouaz, T. Bouhal, A. Allouhi, T. Kousksou, A. Jamil, and Y. Zeraouli, "Energy and parametric analysis of solar absorption cooling systems in various Moroccan climates", Case Studies in Thermal Engineering, Vol. 9, pp. 28-39, March 2017.

[6] M. S. Ahmed, A. Waheed, T. Talha, M. Wajahat, and F. Sarfraz, "Configuration based modeling and performance analysis of single effect solar absorption cooling system in TRNSYS", Energy Convers. Manag., Vol. 157, pp. 351–363, February 2018.

[7] A. Al-Alili, M. D. Islam, I. Kubo, Y. Hwang, and R. Radermacher, "Modeling of a solar powered absorption cycle for Abu Dhabi", Applied Energy, Vol. 93, pp. 160–167, May 2019.

[8] C. Stanciu, D. Stanciu, and A. T. Gheorghian, "Thermal analysis of a solar powered absorption cooling system with fully mixed thermal storage at startup", Energies, MDPI AG, doi:10.3390/en10010072, Vol. 10, No.1, 72, January 2017.

[9] A. A. Al-Ugla, M. A. I. El-Shaarawi, and S. A. M. Said, "Alternative designs for a 24-hours operating solar-powered LiBr–water absorption air-conditioning technology", International Journal of Refrigeration, Vol. 53, pp. 90-100, May 2015.

[10] A. Saeed, M. Zubair, F. A. Khan, M. Siddique, and A. Shiwlani, "Energy Savings through Ammonia Based Absorption Chiller System: A proposed Strategy", 7th International Conference on Renewable Energy Research and Applications, (ICRERA), Paris, France, pp. 168-173, 14-17 October 2018.

[11] C. Naranjo-Mendoza, D. R. Rousse, G. Quesada, "Modeling of a solar absorption cooling system for Guayaquil, Ecuador", 2nd International Conference on Renewable Energy Research and Application (ICRERA), Madrid, Spain, pp. 853-856, 20-23 October 2013.

[12] M. H. Ahmed, M. Rady, A. M. Amin, and F.M. Montagnio, F. Paredes, "Comparison of thermal and optical performance of Linear Fresnel and Parabolic Trough Concentrator", International Conference on Renewable Energy Research and Application (ICRERA), Palermo, Italy, pp. 626-629, 22-25 November 2015.

[13] A. Messadi and Y. Timoumi, "Modeling of the Parabolic Trough Solar Field with Molten Salt for the Region of Tozeur in Tunisia", International Conference on Renewable Energy Research and Application (ICRERA), Paris, France, pp. 993-997, 14-19 October 2018.

[14] M. H. Ahmed, A. Giaconia, and A. M. A. Amin, "Effect of solar collector type on the absorption system performance", International Conference on Renewable Energy Research and Application (ICRERA), San Diego, USA, 5-8 November 2017.

[15] T. He, X. Zhang, C. Wang, M. Wang, B. Li, N. Xue, K. Shimizu, K. Takahashi, and Y. Wuc, "Application of solar thermal cooling system driven by low temperature heat source in China", Energy Procedia, Vol. 70, pp. 454 -461, 2015.

[16] M. Mazloumi, M. Naghashzadegan, and K. Javaherdeh, "Simulation of solar lithium bromide-water absorption cooling system with parabolic trough collector", Energy Convers. Manage, Vol. 49, No. 10, pp. 2820-2832, October 2008.

[17] F. Agyenim, I. Knight, and M. Rhodes, "Design and experimental testing of the performance of an outdoor LiBr/H2O solar thermal absorption cooling system with a cold store", Solar Energy, Vol.84, No. 5, pp.735-744, May 2010.

[18] G. A. Florides, S. A. Kalogirou, S. A. Tassou, and L. C. Wrobel, "Modelling, simulation and warming impact assessment of a domestic-size absorption solar cooling system", Applied Thermal Energy, Vol. 22, No. 12, pp. 1313-1325, August 2002.

[19] S. Fischer, W. Heidemann, H. Müller-Steinhagen, B. Perers, P. Bergquist, and B. Hellström, "Collector test method under quasi-dynamic conditions according to the European Standard EN 12975-2", Solar Energy, Vol. 76, No. 1-3, pp. 117–123, January–March 2004.

[20] M. H. Ahmed, A. M. A. Amin, and H. E. Fath, "Modeling of Solar Power Plant for Electricity Generation and Water Desalination", Journal of Solar Energy Engineering, Vol. 14, 011015, February 2019.